ISSN 2176-5480

22nd International Congress of Mechanical Engineering (COBEM 2013)
November 3-7, 2013, Ribeirão Preto, SP, Brazil

BRAZILIAN 14-X B HYPERSONIC SCRAMJET AEROSPACE VEHICLE ANALYTIC THEORETICAL ANALYSIS AT MACH NUMBER 7

Victor Alves Barros Galvão
Universidade do Vale do Paraíba/UNIVAP, Campus Urbanova Av. Shishima Hifumi, nº 2911 Urbanova CEP. 12244-000 São José dos Campos, SP - Brasil
victorabgalvao@hotmail.com

Paulo Gilberto de Paula Toro
Instituto de Estudos Avançados/IEAv, Trevo Coronel Aviador José Alberto Albano do Amarante, nº 1 Putim CEP. 12.228-001 São José dos Campos, SP, Brasil
toro@ieav.cta.br

Abstract. *The Brazilian 14-X B Hypersonic Aerospace Vehicle, VHA 14-X B, is a vehicle integrated with the hypersonic airbreathing propulsion system based on supersonic combustion (scramjet), designed at the Prof. Henry T. Nagamatsu Laboratory of Aerothermodynamics and Hypersonics, to demonstrate at Earth's atmospheric free-flight at 30km altitude at Mach number 7. Scramjet technology offers substantial advantages to improve performance of aerospace vehicle that flies at hypersonic speeds through the Earth's atmosphere, by reducing onboard fuel. Basically, scramjet is a fully integrated airbreathing aeronautical engine that uses the oblique/conical shock waves generated during the hypersonic flight, to promote compression and deceleration of freestream atmospheric air at the inlet of the scramjet. Fuel, at least sonic speed, may be injected into the supersonic airflow just downstream of the inlet. Right after, both atmosphere air and on-board hydrogen fuel are mixing. The combination of the high energies of the fuel and the oncoming hypersonic airflow the combustion at supersonic speed starts. Analytic theoretical analysis, computational fluid dynamics simulation and experimental investigation are the methodologies used to design a technological demonstrator, before flight thoughout Earth's atmosphere. Thermodynamics properties (pressure, temperature, density, sound velocity) at external inlet lower surfaces, scramjet power off and power on internal surfaces, and external outlet lower surfaces will be obtain based on theoretical analysis using two-dimensional oblique shock wave compressible flow, one-dimensional flow with heat addition and Prandtl-Meyer theories, respectively.*

Keywords: VHA 14-X B, hypersonic airbreathing propulsion, scramjet, waverider, hypersonic shock tunnel

1. THE BRAZILIAN 14-X B HYPERSONIC AEROSPACE VEHICLE

The VHA 14-X B (Fig. 1) is being designed at the Prof. Henry T. Nagamatsu Laboratory of Aerothermodynamics and Hypersonics, at the Institute for Advanced Studies (IEAv) since March 2012, as an option to demonstrate the hypersonic airbreathing propulsion system based on supersonic combustion at free flight at 30km altitude at Mach number 7, using Brazilian two-stage rocket engines (S31 and S30), which are able to boost the VHA 14-X B to the predetermined conditions of the scramjet operation, 30km altitude but at Mach number 7.

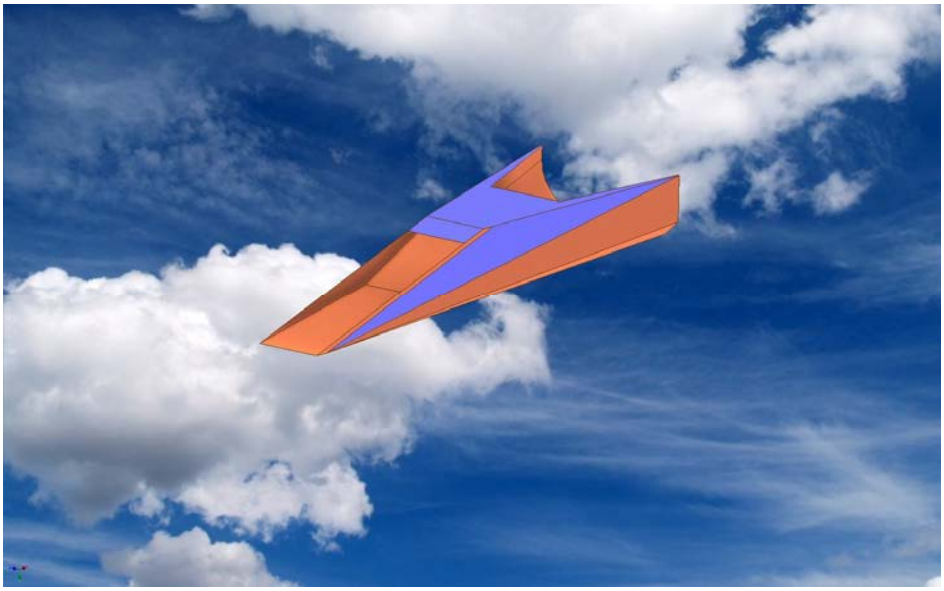

Figure 1: 14-X B Hypersonic Aerospace Vehicle, VHA 14-X B.

ISSN 2176-5480

The VHA 14-X B (Fig. 1) consists a two-dimensional configuration, with a constant cross-section (Fig. 2), where the upper flat surface, with zero angle of attack, is aligned with the freestream Mach number 7 hypersonic airflow. The lower surface, taken from the VHA 14-X waverider external configuration (Rolim, 2009; Rolim et al., 2009; Rolim et al., 2011; Costa, 2011; Costa et al., 2012) consists of a frontal surface with a leading edge angle of 5.5^o, compression ramp angle of 14.5^o (related to the angle of the leading edge), the internal expansion chamber combustion angle of 4.27^o and external expansion angle of 10.73^o (related to the angle of internal expansion). The cross-section height is $165-mm.$. The combustor chamber $258.63-mm.$ long with constant area, following by $134-mm.$ long with 4.27^o (to accommodate the boundary layer and expansion due H_2 and O_2 combustion) was defined by research of the Hyslop (1998) and Kasal et al. (2002), respectively. The constant area combustion chamber is $15.2-mm.$ high (to accommodate the airflow captured by the VHA 14-X B frontal area).

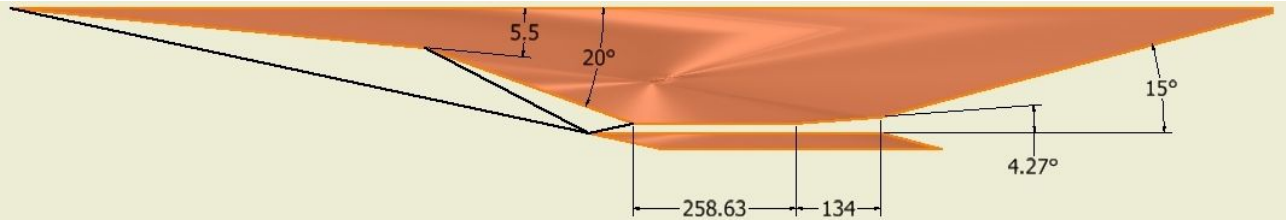

Figure 2: Cross-section of the V14-X B.

Analytic theoretical analysis, computational fluid dynamics simulation and experimental investigation are the methodologies used to design a technological demonstrator, before flight throughout Earth's atmosphere. Two-dimensional steady state, non-viscous, no heat conduction compressible flow applied to the shock and expansion waves may be used as analytic theoretical analysis. Available commercial CFD codes are able to investigate numerically the turbulent real gas hypersonic airflow under combustion process. Reflected hypersonic shock tunnels are ground-based experimental facilities capable to duplicate the flight conditions.

Analytic theoretical analysis may be used as first step to calculate the thermodynamics properties (pressure, temperature, density, sound velocities, among others) at the lower surface of hypersonic vehicle with airframe-integrated scramjet engines.

First it is necessary to establish a nomenclature to be used in the analytic theoretical analysis. Following Heiser and Pratt (1994) the VHA 14-X B may be divided in three (Fig. 3) main components: external and internal compression section (inlet), combustion chamber (combustor) and internal and external expansion section (outlet). Also, the hypersonic vehicle with airframe-integrated scramjet engine lower surface may be divided by several stations (Fig. 3).

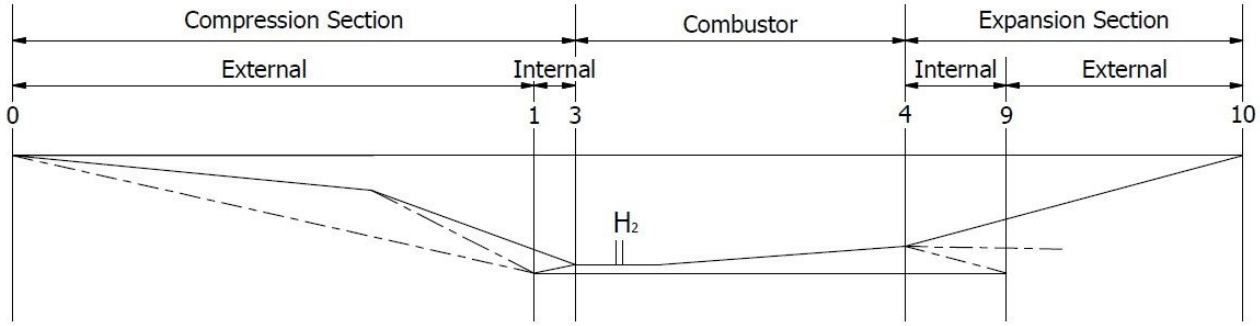

Figure 3: Hypersonic vehicle with airframe-integrated scramjet engine stations and reference terminology.

2. ANALICTIC THEORETICAL ANALYSIS

In this analytic theoretical analysis, the subscripts *in* and *out* are used to identify the upstream (inlet) and the downstream (outlet) conditions, respectively, of the each station (Fig. 3) of the hypersonic vehicle with airframe-integrated scramjet engine lower surface.

2.1 External and Internal Compression Section (Oblique Shock Wave)

Mass, momentum and energy conservation laws (Anderson, 2003) in two-dimensional steady state, non-viscous, no heat conduction compressible flow, applied to oblique shock waves (Fig. 4), are given by:

ISSN 2176-5480

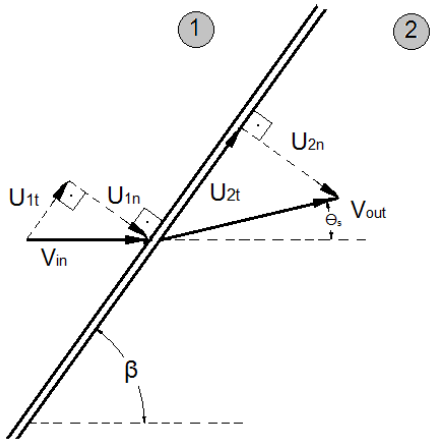

Figure 4: Leading edge incident Oblique Shock wave geometry.

$$\rho_{in}\, u_{in_n} = \rho_{out}\, u_{out_n} \tag{1}$$

$$p_{in} + \rho_{in} u_{in_n}^2 = p_{out} + \rho_{out} u_{out_n}^2 \tag{2}$$

$$u_{in_t} = u_{out_t} \tag{3}$$

$$h_{in} + \frac{u_{in_n}^2}{2} = h_{out} + \frac{u_{out_n}^2}{2} \tag{4}$$

where: ρ, p, u_n, u_t, h are density, pressure, normal and tangential velocities across the oblique shock wave and enthalpy of the gas, respectively.

For calorically and/or thermally perfect gas ($p = \rho RT$, $\gamma = \text{constant}$) the oblique shock relationships can be easily obtained as closed form of the thermodynamics property (static pressure, static density and static temperature) rations and Mach number across the oblique shock given by:

$$\frac{p_{out}}{p_{in}} = 1 + \frac{2\gamma}{(\gamma+1)}\left[\left(M_{in}\, sen\beta\right)^2 - 1\right] \tag{5}$$

$$\frac{\rho_{out}}{\rho_{in}} = \frac{(\gamma+1)\left(M_{in}\, sen\beta\right)^2}{\left[(\gamma-1)\left(M_{in}\, sen\beta\right)^2 + 2\right]} \tag{6}$$

$$\frac{T_{out}}{T_{in}} = \frac{p_{out}}{p_{in}}\ \frac{\rho_{in}}{\rho_{out}} = 1 + \frac{2\gamma}{(\gamma+1)}\left[\left(M_{in}\, sen\beta\right)^2 - 1\right]\ \frac{\left[(\gamma-1)\left(M_{in}\, sen\beta\right)^2 + 2\right]}{(\gamma+1)\left(M_{in}\, sen\beta\right)^2} \tag{7}$$

$$M_{out} = \frac{\sqrt{\dfrac{\left(M_{in}\, sen\beta\right)^2 + \dfrac{2}{(\gamma-1)}}{\dfrac{2\gamma}{(\gamma-1)}\left(M_{in}\, sen\beta\right)^2 - 1}}}{sen\left(\beta - \theta_s\right)} \tag{8}$$

where: θ_s , β are the deflection and shock wave angles, respectively.

Additionally, the shock wave angle β with respect to the local flow direction θ_s may be obtained iteratively with the relationship given by:

ISSN 2176-5480

$$tg\theta_s = 2(\text{cotg}\,\beta)\left[\frac{(M_{in}\ sen\beta)^2 - 1}{M_{in}^2(\gamma + \cos 2\beta) + 2}\right] \tag{9}$$

Note, the flow across the oblique shock wave promote an increase of pressure, density, temperature, and a decrease of Mach number, however the flow remains supersonic/hypersonic and parallel to the flat surface of the external and internal compression section (Fig. 5) of the hypersonic vehicle with airframe-integrated scramjet engine lower surface.

Also, the leading edge incident Oblique Shock wave methodology may be used for incident oblique planar (Fig. 5) shock wave (compression ramp angle of 14.5^o, Fig. 3) and the reflected shock wave (Fig. 6).

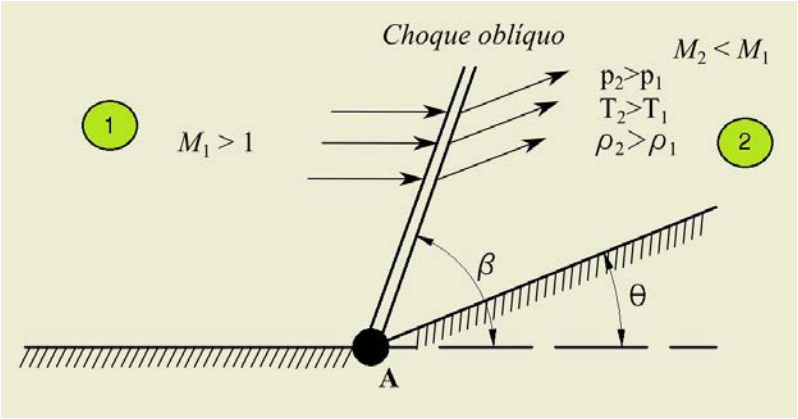

Figure 5: Incident Oblique Shock wave planar geometry.

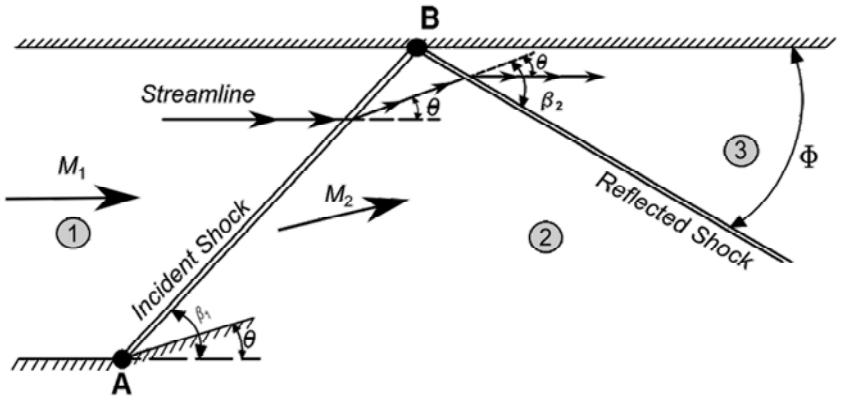

Figure 6: Reflected Oblique Shock wave geometry.

2.2 Combustor Section (One-Dimensional Flow with Heat Addition)

One-dimensional with constant-area heat addition, Rayleigh Flow, (Fig. 7) may be applied to combustion processes between the entrance (inlet) and the exit (outlet) of the scramjet combustor (Fig. 3), where the combustion processes correspond to heat addition at constant pressure, constant density, constant temperature and constant Mach number, respectively, at the inlet of the scramjet combustor. Mass, momentum and energy conservation laws (Anderson, 2003) may be applied to the one-dimensional with constant-area heat addition, and they are given by:

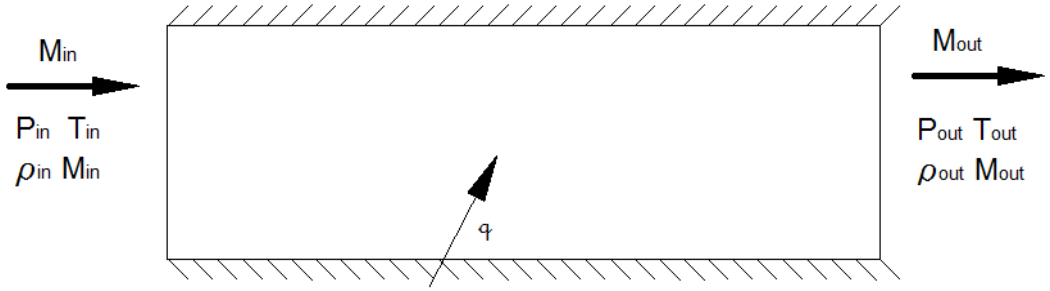

Figure 7: Rayleigh Flow, one-dimensional with constant-area heat addition.

ISSN 2176-5480

$$\rho_{in}\, u_{in} = \rho_{out}\, u_{out} \tag{10}$$

$$p_{in} + \rho_{in}\, u_{in}^2 = p_{out} + \rho_{out}\, u_{out}^2 \tag{11}$$

$$h_{in} + \frac{u_{in}^2}{2} + q = h_{out} + \frac{u_{out}^2}{2} \tag{12}$$

The energy equation (Eq. 12) indicates the heat addition change the total energy (temperature). For calorically and/or thermally perfect gas ($p = \rho RT$, $\gamma = \text{constant}$) and applying the total temperature definition, obtain

$$q = c_p\left(T_{o,\,out} - T_{o,\,in}\right) \tag{13}$$

where: the total temperature is given by:

$$\frac{T_o}{T} = 1 + \frac{\gamma - 1}{2} M^2 \tag{14}$$

Closed form of the thermodynamics property (static pressure, static density and static temperature) rations across constant-area heat addition may be obtained by manipulating the momentum equation, and they are given by:

$$\frac{p_{out}}{p_{in}} = \left(\frac{1 + \gamma\, M_{in}^2}{1 + \gamma\, M_{out}^2}\right) \tag{15}$$

$$\frac{\rho_{out}}{\rho_{in}} = \left(\frac{1 + \gamma\, M_{out}^2}{1 + \gamma\, M_{in}^2}\right) \left(\frac{M_{in}}{M_{out}}\right)^2 \tag{16}$$

$$\frac{T_{out}}{T_{in}} = \left(\frac{1 + \gamma\, M_{in}^2}{1 + \gamma\, M_{out}^2}\right)^2 \left(\frac{M_{out}^2}{M_{in}^2}\right)^2 \tag{17}$$

$$\frac{T_{o,out}}{T_{o,in}} = \left(\frac{1 + \gamma\, M_{in}^2}{1 + \gamma\, M_{out}^2}\right)^2 \left(\frac{M_{out}^2}{M_{in}^2}\right)^2 \left(\frac{1 + \frac{\gamma - 1}{2} M_{out}^2}{1 + \frac{\gamma - 1}{2} M_{in}^2}\right) \tag{18}$$

Note the flow from the external and internal compression section are deflected to the combustor entrance (Fig. 3) at supersonic speed (at constant pressure, constant density, constant temperature and constant Mach number). Fuel (H_2) will be injected right after the entrance station (Fig. 3) in (minimal) sonic speed. Rayleigh flow (one-dimensional flow with heat addition) may be applied to the combustion process to burn H_2 and O_2 in supersonic speed, resulting at the exit of the combustor chamber (outlet) an increase in static pressure, static density, static temperature, reducing the Mach number.

2.3 Internal and External Expansion Section (Expansion Wave)

The Prandtl-Meyer theory may be applied to the (internal and external expansion section, Fig. 3) expansion waves (Fig. 8). An isentropic expansion wave is limited by the head and tail of the expansion wave defined by the Mach angle μ_{head} , μ_{tail} , respectively, and they are given by:

ISSN 2176-5480

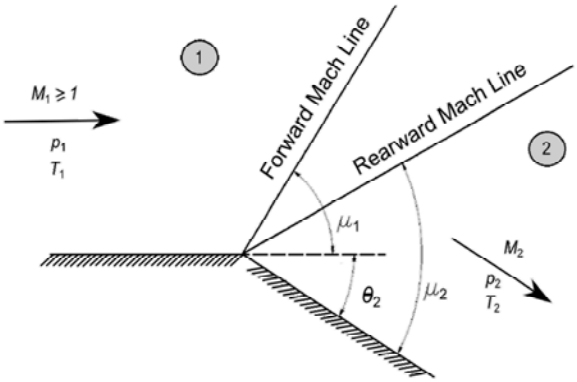

Figure 8: Expansion wave geometry.

$$\mu_{head} = \text{arcsen}\left(\frac{1}{M_{in}}\right) \tag{19}$$

$$\mu_{tail} = \text{arcsen}\left(\frac{1}{M_{out}}\right) \tag{20}$$

The expansion deflection angle θ_e is given by the Prandtl-Meyer function $\upsilon(\mathrm{M})$:

$$\theta_e = \upsilon\left(M_{out}\right) - \upsilon\left(M_{in}\right) \tag{21}$$

where the Prandtl-Meyer function $\upsilon(\mathrm{M})$, which is function of the Mach number, is given by:

$$\upsilon(M) = \sqrt{\frac{\gamma+1}{\gamma-1}}\ tg^{-1}\sqrt{\frac{\gamma-1}{\gamma+1}\left[M^2-1\right]} - tg^{-1}\sqrt{M^2-1} \tag{22}$$

Once Mach number after expansion wave $\mathrm{M}_{\mathrm{out}}$ is determined the closed form of the thermodynamics property (static pressure, static density and static temperature) rations across the expansion wave may be obtained by the isentropic relationships given by:

$$\frac{T_{out}}{T_{in}} = \left(\frac{1+\frac{\gamma-1}{2}M_{in}^2}{1+\frac{\gamma-1}{2}M_{out}^2}\right) \tag{23}$$

$$\frac{p_{out}}{p_{in}} = \left(\frac{T_{out}}{T_{in}}\right)^{\frac{\gamma}{\gamma-1}} \tag{24}$$

$$\frac{\rho_{out}}{\rho_{in}} = \frac{p_{out}}{p_{in}}\frac{T_{in}}{T_{out}} \tag{25}$$

Note the flow across the expansion wave promote a decrease of static pressure, static density, static temperature, and an increase of Mach number. The flow remains supersonic/hypersonic and parallel to the flat surface of the internal and external expansion section (Fig. 3) of the hypersonic vehicle with airframe-integrated scramjet engine lower surface.

3. RESULTS AND COMMENTS

Four test cases related to the two-dimensional configuration of the VHA 14-X B (Fig. 2) using the reference terminology (Fig. 3), flying at 30km altitude at Mach number 7 are presented for:

ISSN 2176-5480

- Case 1) Analytic theoretical analysis applied to the complete VHA 14-X B lower surface, considering the simplest case, i. e., no viscous flow, calorically perfect air ($\gamma = 1.4$) and scramjet engine with power off (Table 1).
- Case 2) Analytic theoretical analysis applied to the complete VHA 14-X B lower surface with no viscous flow and power off at the scramjet engine, but considering the thermodynamic properties of the air are in chemical equilibrium, with variable γ (Table 2).
- Case 3) Analytic theoretical analysis applied to the complete VHA 14-X B lower surface considering the boundary effects (viscous flow) with power off at the scramjet engine and the thermodynamic properties of the air in chemical equilibrium, with variable γ (Table 3).
- Case 4) Analytic theoretical analysis applied to the complete VHA 14-X B lower surface considering the boundary effects (viscous flow), power on (burning H_2 and O_2) at the scramjet engine and the thermodynamic properties of the air in chemical equilibrium, with variable γ (Table 4).

In all cases, the standard atmospheric properties at 30km altitude (U.S. standard Atmosphere, 1976) are given as $p = 1197(Pa)$, $T = 226.5(K)$, $\rho = 0.01841(kg/m^3)$, $a = 301{,}7(m/s)$, where a is sound velocity.

Note that in all four cases, the incident shock waves generated at the 5.5° attached leading-edge deflection angle and at the 14.5° deflection (following the leading-edge deflection) hit the cowl leading-edge. The reflected shock wave generated at the cowl leading-edge hits the entrance of the combustor station (Fig. 3).

Also, in the three first cases, the flow from the external and internal compression section are deflected to the combustor entrance (Fig. 3) at supersonic speed (at constant pressure, constant density, constant temperature and constant Mach number) and remains constant at the exit of the combustor.

Additionally, for the case four the one-dimensional flow with heat addition is considered at the combustor section.

Finally, for all four cases, the closed form of the thermodynamics property (pressure, density and temperature) rations and Mach number across the oblique shock waves and expansion waves are applied to the external and internal compression section and the internal and external expansion section (Fig. 3), respectively.

Case 1) Analytic theoretical analysis applied to the complete VHA 14-X B lower surface, considering the simplest case, i. e., no viscous flow, calorically perfect air ($\gamma = 1.4$) and scramjet engine with power off (Table 1).

Basically, the first step is to apply the most simple case, which means no heat addition at the combustor section, only oblique and reflected shock waves (Eqs. 5-9) and expansion waves (Eqs. 19-25) calculations considering no viscous flow (boundary layer), calorically perfect (no dissociations) air supersonic/hypersonic flow.

Table 1: Thermodynamic properties at the VHA 14-X B lower surfaces, power off, inviscid, $\gamma = 1.4$.

		station 0	station 1 (deflection 5.5º)	station 2 (deflection 14.5º)	station 3 (deflection 20º)	station 4 (Power off) (deflection 4.27º)	station 4 (deflection 10.73º)
M_{in}		7	7	6.0188	4.0645	2.6012	2.7981
θ_{in}	º		5.5	14.5	20	4.27	10.73
β_{out}	º		12.2429	22.1143	32.2384		
M_{out}			6.0188	4.0645	2.6012	2.7981	3.3715
T_{out}	K	226.5	296.6924	568.3735	1039.555	953.2721	747.1747
p_{out}	Pa	1197	2877.588	16755.91	89104.56	65803.72	28052.13
ρ_{out}	kg/m^3	0.01841	0.033788	0.102702	0.298605	0.240467	0.13079
a_{out}	m/s	301.7	345.9846	478.8732	647.6307	620.1719	549.0535
u_{out}	m/s	2111.9	2082.412	1946.38	1684.617	1735.303	1851.134
μ_{head}	º					22.6107	20.9405
μ_{tail}	º					20.9394	17.2536

Case 2) Analytic theoretical analysis applied to the complete VHA 14-X B lower surface with no viscous flow and power off at the scramjet engine, but considering the thermodynamic properties of the air are in chemical equilibrium, with variable γ (Table 2).

ISSN 2176-5480

In this preliminary calculation a simple iterative procedure to evaluate γ is used to account for the chemical equilibrium airflow effects.

Observe, the airflow compressed by the 5.5° attached leading-edge deflection angle may be considered as calorically perfect gas (Table 1), while due the temperatures higher than 400 K approximately (Table 1) the ratio of specific heats γ decrease as function of temperature.

This behavior is anticipated by Heiser and Pratt (1994), therefore these data (Fig. 9) must applied in the closed form of the thermodynamics property rations and Mach number across the oblique shock waves and expansion waves. More sophisticated models of chemical equilibrium airflow must be developed.

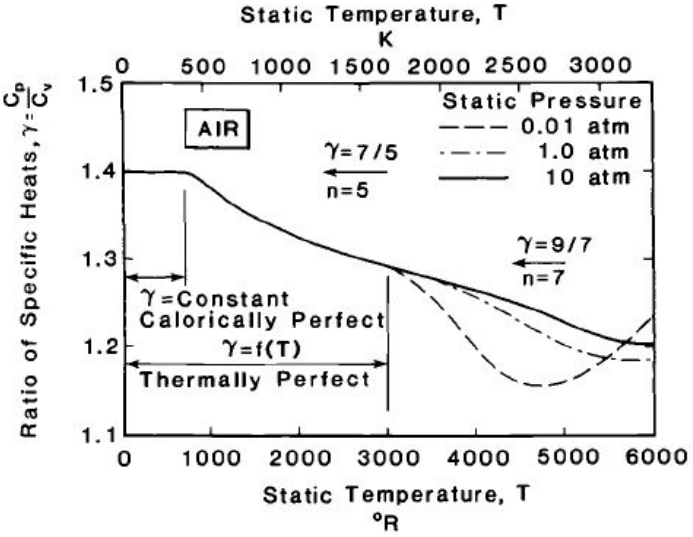

Figure 9: Equilibrium ratio of specific heats of air (Heiser and Pratt, 1994).

Table 2: Thermodynamic properties at the VHA 14-X B lower surfaces, power off, inviscid, γ = variable .

		station 0	station 1 (deflection 5.5º)	station 2 (deflection 14.5º)	station 3 (deflection 20º)	station 4 (Power off) (deflection 4.27º)	station 4 (deflection 10.73º)
		1.4	1.3985	1.3798	1.3396	1.3457	1.3643
M_{in}		7	7	6.0217	4.1272	2.7552	2.9464
θ_{in}	º		5.5	14.5	20	4.27	10.73
β_{out}	º		12.2399	21.9738	31.389		
M_{out}			6.0217	4.1272	2.7552	2.9464	3.516
T_{out}	K	226.5	296.3979	551.9522	937.8219	867.0164	688.1509
p_{out}	Pa	1197	2875.314	16468.65	84755.89	62456.62	26281.74
ρ_{out}	kg/m^3	0.01841	0.033795	0.103944	0.314846	0.250964	0.133036
a_{out}	m/s	301.7	345.6276	468.4879	601.7102	579.8656	520.1593
u_{out}	m/s	2111.9	2081.266	1933.543	1657.832	1708.516	1828.88
μ_{head}	º					21.2831	19.843
μ_{tail}	º					19.8399	16.5238

Chemical equilibrium airflow effects are considered in all sections by manually interactions. The thermodynamic properties are calculated for the specific sections (ex.: section 1).

First, the specific heats of air γ is evaluated for a given static pressure and static temperature. Next, the shock wave angle β with respect to the local flow direction θ_s is obtained iteratively (Eq. 9). Finally, thermodynamic properties are calculated (Eqs. 5 to 7).

The specific heat of air γ is evaluated again for new values of the static pressure and static temperature. This procedure is applied until there is no difference of the specific heats of air γ between two consecutive interactions.

ISSN 2176-5480

Case 3) Analytic theoretical analysis applied to the complete VHA 14-X B lower surface considering the boundary effects (viscous flow) with power off at the scramjet engine and the thermodynamic properties of the air in chemical equilibrium, with variable γ (Table 3).

The Chapman-Rubesin (Chapman et al., 1958) theory describes the calculation of the displacement thickness δ^*. It may predict the viscous effects on the external and internal compression section lower surfaces. This boundary layer may be included virtually at the 5.5° attached leading-edge deflection angle and at the 14.5° deflection angle (Fig. 10).

Due the low supersonic Mach number at the combustion chamber (Tables 2 and 3) the displacement thickness δ^* is considered negligible. It was applied at the external and internal compression sections only.

Based on Chapman-Rubesin theory displacement thickness δ^* was applied to the 5.5° attached leading-edge deflection and to the 14.5° deflection angles. Due to 4.4mm in 0.67m and 1.2 in 0.57m, the angles were increase to 5.9594° and 14.7349°, respectively. The closed form of the thermodynamics property rations and Mach number across the oblique shock waves were applied to the 5.9594° leading-edge deflection and to the deflection 14.7349° angles (Table 3).

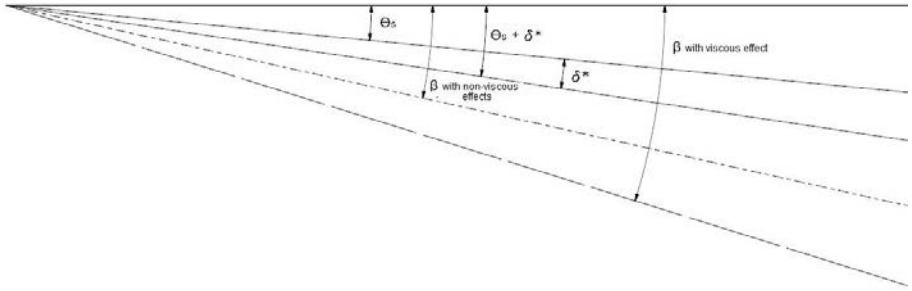

Figure 10: Displacement thickness δ^* to account for the viscous effects.

Table 3: Thermodynamic properties at the VHA 14-X B lower surfaces, power off, viscous effects, γ = variable .

		station 0	station 1 (deflection 5.5º)	station 2 (deflection 14.5º)	station 3 (deflection 20º)	station 4 (Power off) (deflection 4.27º)	station 4 (deflection 10.73º)
		1.4	1.3984	1.3783	1.3385	1.3457	1.3643
M_{in}		7	7	5.9419	4.0642	2.7552	2.9464
θ_{in}	º		5.9594	14.7349	20	4.27	10.73
β_{out}	º		12.6315	22.3161	31.588		
M_{out}			5.9419	4.0642	2.7252	2.9464	3.516
T_{out}	K	226.5	303.4194	564.8456	949.9573	878.2355	697.0555
p_{out}	Pa	1197	3071.861	17636.48	88946.04	65544.34	27581.06
ρ_{out}	kg/m^3	0.01841	0.03527	0.108772	0.326186	0.260003	0.137828
a_{out}	m/s	301.7	349.685	473.6705	605.342	583.6053	523.5139
u_{out}	m/s	2111.9	2077.793	1925.092	1649.678	1719.535	1840.675
μ_{head}	º					21.2831	19.843
μ_{tail}	º					19.8399	16.5238

Case 4) Analytic theoretical analysis applied to the complete VHA 14-X B lower surface considering the boundary effects (viscous flow), power on (burning H_2 and O_2) at the scramjet engine and the thermodynamic properties of the air in chemical equilibrium, with variable γ (Table 4).

The stoichiometric ratio f_{st} of H_2 and O_2 is calculated from the basic principles of chemical reactions using

ISSN 2176-5480

$$f_{st} = \frac{36x + 3y}{103(4x + y)} \tag{26}$$

where x = 0 and y = 2 for H_2. Therefore, $f_{st} = 0.0291$ $\left(\text{to burn } H_2 \text{ and } O_2\right)$.

Also, f_{st} may be calculated based on the mass flow rate ratio, given by

$$f_{st} = \frac{\dot{m}_{\text{fuel}}}{\dot{m}_{\text{air}}} \tag{27}$$

Therefore, the fuel mass flow may be calculated as $\dot{m}_{fuel} = f_{st}\ \dot{m}_{air}$, where $\dot{m}_{air} = \rho_0\ u_0\ A_0 = \rho_3\ u_3\ A_3$.

The rate at which the chemical reactions make energy available to the combustor is given by Chemical energy rate = $\dot{m}_{\text{fuel}}\ h_{pr}$ (Heiser and Pratt, 1994).

However, the amount of heat added per kilogram of air is proportional to the fuel to air mass flow ratio and the heat of reaction h_{pr} of the fuel, which may be evaluated by

$$q = f_{st} h_{pr} = \frac{\dot{m}_{\text{fuel}}}{\dot{m}_{\text{air}}}\ h_{pr} \tag{28}$$

where, the heat of reaction h_{pr} of the H_2 is 119.954 MJ/kg.

Curran et al. (1996) recommends the maximum heat added to burn H_2 may be calculated by

$$\left(\frac{q}{c_p T}\right)_{\max} = \frac{\left(M_{in}^2 - 1\right)^2}{2(\gamma + 1)\ M_{in}^2} \tag{29}$$

where, q is the heat addition per mass unity [J/kg], γ is the ratio of specific heats, c_p is the specific heat at constant pressure [J/kg-K], T is the temperature [K] and M_{in} is the Mach number. All properties are evaluated at the combustor inlet conditions (before the fuel injection), then

$$q_{\max}^{\text{at combustor inlet conditions}} = \frac{\left(M_{in}^2 - 1\right)^2}{2(\gamma + 1)\ M_{in}^2} c_p T \tag{30}$$

where for the case 4, c_p is 1139.2 [J/kg-K] at 88.946 [Pa] and 949.96 [K], which indicates 35% of the chemical energy rate available stoichiometrically to the combustor. Therefore, it is necessary to adjust the injection of the H_2 in order to prevent the choking flow at the end of the combustor, which may include in the parameter $f_{H_2\ adjust}$,

$$f_{H_2\ adjust} = \frac{q_{\max}^{at\ combustor\ inlet\ conditions}}{f_{st} h_{pr}} \tag{31}$$

Finally, the amount of heat added per kilogram of air is proportional to the fuel to air mass flow ratio, the heat of reaction h_{pr} of the fuel and the parameter $f_{H_2\ adjust}$, which may be evaluated by

ISSN 2176-5480

$$q = f_{H_2\ \text{adjust}}\ f_{st}\ h_{pr} = f_{H_2\ \text{adjust}}\ \frac{\dot{m}_{\text{fuel}}}{\dot{m}_{\text{air}}}\ h_{pr} \tag{32}$$

The heat addition changes the total energy (temperature) $q = c_p\left(T_{o,\,out} - T_{o,\,in}\right)$, from the total temperature at the entrance to the total temperature at the exit of the combustor. Consequently, increase the static pressure (Eq. 15), static density (Eq. 16), static temperature (Eq. 17), and reducing the Mach number at the exit of the combustor, where $1 < M_{out} < M_{in}$ at the combustor section. Note, the heat addition drives the Mach number towards 1. When the flow become sonic the flow is called choking because the amount of heat added is higher than necessary to burn the fuel. Therefore, the fuel mass flow rate must be adjusted to prevent the choke limit.

Table 4: Thermodynamic properties at the VHA 14-X B lower surfaces, power on, viscous effects, γ = variable .

		station 0	station 1 (deflection 5.5º)	station 2 (deflection 14.5º)	station 3 (deflection 20º)	combustor (Raleigh Flow)	station 4 (Power off) (deflection 4.27º)	station 4 (deflection 10.73º)
		1.4	1.3984	1.3783	1.3385	1.3385	1.4	1.4
M_{in}		7	7	5.9419	4.0642	2.7252	1.173	1.3364
θ_{in}	º		5.9594	14.7349	20		4.27	10.73
β_{out}	º		12.6315	22.3161	31.588			
M_{out}			5.9419	4.0642	2.7252	1.173	1.3364	1.7030
T_{out}	K	226.5	303.4194	564.8456	949.9573	2608.9189	2451.3402	2105.2109
p_{out}	Pa	1197	3071.861	17636.48	88946.04	342448.03	275328.2161	161645.1956
ρ_{out}	kg/m^3	0.01841	0.03527	0.108772	0.326186	0.45729	0.391303	0.26749
a_{out}	m/s	301.7	349.685	473.6705	605.342	1002.67	994.10	921.31
u_{out}	m/s	2111.9	2077.793	1925.092	1649.678	1176.13	1328.52	1568.99
μ_{head}	º						58.4863	48.4609
μ_{tail}	º						48.4409	35.9591

4. CONCLUSION

The primary objective of this work is to present a methodology to design a hypersonic vehicle with airframe-integrated scramjet engine using the analytic theoretical analysis based on the two-dimensional oblique shock wave compressible flow, one-dimensional flow with heat addition and Prandtl-Meyer theory, applied to the Brazilian vehicle integrated with the hypersonic airbreathing propulsion system based on supersonic combustion (scramjet), VHA 14-X B, in four cases: 1) no viscous flow, calorically perfect air ($\gamma = 1.4$) and power off scramjet engine; 2) no viscous flow, air in chemical equilibrium (variable γ) and power off scramjet engine; 3) viscous flow, air in chemical equilibrium (variable γ) and power off scramjet engine; and 4) boundary effects (viscous flow), air in chemical equilibrium (variable γ) and power on (burning H_2 and O_2) at the scramjet engine.

Indeed, the Brazilian VHA 14-X B is a technological demonstrator of a hypersonic airbreathing propulsion system based on supersonic combustion (scramjet) to fly at Earth's atmosphere at 30km altitude at Mach number 7, designed at the Prof. Henry T. Nagamatsu Laboratory of Aerothermodynamics and Hypersonics, at the Institute for Advanced Studies. Basically, scramjet is an aeronautical engine, without moving parts, therefore it is necessary another propulsion system to accelerate the scramjet to the operation conditions. Rocket engines are a low-cost solution to launch scramjet integrated vehicle to flight to the test conditions. It is intent, in the near future to use the Brazilian two-stage rocket engines (S31 and S30) to boost the VHA 14-X B to the predetermined conditions of the scramjet operation, 30km altitude at Mach number 7.

ISSN 2176-5480

5. ACKNOWLEDGEMENTS

The second author would like to express gratitude to FINEP (agreement nº 01.08.0365.00, project nº 0445/07) for the financial support for the 14-X Hypersonic Aerospace Vehicle design and experimental investigations; and to CNPq (project nº 520017/2009-9) for the financial support to undergraduate students.

Also, the first author acknowledges the CNPq (grant # 183691/2009-1) for financial support to undergraduate student.

6. REFERENCES

Anderson Jr., J. A. "Modern Compressible Flow, The Historical Perspective" McGraw-Hill, Inc, 2003.

Chapman D.R., Kuehn D.M. and Larson H.K., Investigation of Separated Flows in Supersonic and Subsonic Streams with Emphasis on the Effect of Transition, NACA report No. 1356, 1958.

Costa, F.J. "Projeto Dimensional para Manufatura do Veículo Hipersônico Aeroespacial 14-X" (in Portuguese). Undergraduate Work, FATEC de São José dos Campos: Professor Jessen Vidal, Brazil, 2011.

Costa, F.J., Toro, P.G.P., Rolim. T.C., Camilo, G.C., Follador, R.C. and Minucci, M.A.S., "Design of the Brazilian Hypersonic waverider Aerospace Vehicle", 14th Brazilian Congress of Thermal Sciences and Engineering, October 18-22, 2012, Rio de Janeiro, RJ, Brazil

Curran, E. T., Heiser, W. H. and Pratt, D. T. "Fluid Phenomena in Scramjet Combustion Systems". Annual Review Fluid Mechanics, vol. 28, pp. 323-360, 1996.

Heiser, H. W. and Pratt, D. T (with Daley, D. H. and Mehta, U. B.). Hypersonic Airbreathing Propulsion. Education Series. EUA. AIAA. 1994.

Hyslop, P. "CFD Modeling of Supersonic Combustion in a scramjet Engine". Doctoral Thesis. The Australian National University, 1998.

Kasal, P, Gerlinger, P., Walther, R., Wolfersdorf, J. V. and Weigand, B. "Supersonic Combustion: Fundamental Investigations of Aerothermodynamic Key Problems". AIAA-2002-5119, 2002.

Rolim, T. C., "Experimental Analysis of a Hypersonic Waverider", M.Sc. Thesis (in English), Instituto Tecnológico de Aeronáutica, São José dos Campos, Brazil, 2009.

Rolim, T. C., Minucci, M. A. S., Toro, P. G. P. and Soviero, P. A. O., "Experimental Results of a Mach 10 Conical-Flow Derived Waverider". 16th AIAA/DLR/DGLR International Space Planes and Hypersonic Systems and Technologies Conference. AIAA 2009-7433, 2009.

Rolim, T.C., Toro, P.G.P., Minucci, M.A.S, Oliveira, A.C. and Follador, R.C., 2011, "Experimental results of a Mach 10 conical-flow derived waverider to 14-X hypersonic aerospace vehicle". Journal of Aerospace Technology and Management, São José dos Campos, Vol.3, No.2, pp. 127-136, May-Aug., 2011.

U.S. Standard Atmosphere, 1976. NASA TM-X 74335. National Oceanic and Atmospheric Administration, National Aeronautics and Space Administration and United States Air Force.

7. RESPONSIBILITY NOTICE

The authors are the only responsible for the printed material included in this paper.